Degradation of Aluminide Layers During Cyclic Oxidation of Ferritic 430 Stainless Steel

Mohammad Badaruddin
Department of Mechanical Engineering, Lampung University, Bandar Lampung
Email: rudin_ntust@yahoo.com

ABSTRACT

In order to increase the performance of the preferred Ferritic 430 SS for manufacturing automobile and motor-cycle exhaust systems. The aluminizing coating on the surface of bare steel was applied by hot-dipping method in a molten pure aluminum. The high temperature oxidation of the aluminized steel was cyclically studied at 900 °C and 1000 °C in static air. The degradation of intermetallic layers during cyclic oxidation were analyzed by means of X-ray Diffraction (XRD), Scanning Electron Microscopy (SEM) and Energy Dispersive Spectroscopy (EDS). The crack perpendicular to the specimen surface rapidly propagated through the FeAl and Fe_3Al layers due to a thermal expansion mismatch upon cooling to room temperature. The accumulation of voids generated crack at the interface between the aluminide layer and the steel substrate. Oxygen is allowed to penetrate into the aluminide layer crack, rapidly forming alumina oxide and closing the crack. Some of the aluminide layers peeled off due to this rapid growth. Thus, the protective Al_2O_3 layer degraded and later, the substrate was oxidized subsequently to form iron-rich oxide (Fe_2O_3) at 1000 °C.

Keywords: Ferritic 430 stainless steel, cyclic oxidation, aluminide layer.

INTRODUCTION

Ferritic 430 stainless steel (SS430) is widely used as an exhaust material in petrochemical, gasification and automotive application because it has a cheaper price than austenitic stainless steel. However, the oxidation resistance of ferritic SS430 is not sufficient for sustainably used at 1000 °C for long time exposure [1]. The high temperature application of this stainless steel has some limitation due to the formation of unprotective Fe_2O_3 layer, which leads to breakaway oxidation and results in metal loss [2,3]. For improving high-temperature oxidation resistance of the steel, several of coating processes; hot-dipping process is an effective and inexpensive method to modify on the surface of bare steel because its process is simpler and it provides a thick coating layer for reliable oxidation resistance [4–6].

The inward diffusion of Al into steel substrate at temperatures above 900 °C forms the inter-metallic compounds FeAl and Fe_3Al [7]; this consequently reduces the solubility of Cr to a lower level in the aluminide layer compared to in the metal substrate. Some studies report that the FeAl and Fe_3Al alloys without Cr show a decrease in oxidation resistance at 1000 °C [8,9]. Lee et al. reported that the addition of 2-4 % Cr first decreases the oxidation resistance of Fe_3Al alloys, but then increases it with further addition of Cr (up to 6 %) [10]. Chromium was found to be the most effective element in improving the high temperature ductility of FeAl and Fe_3Al [11]. In addition, the formation of a protective layer of Al_2O_3 is also promoted. Therefore, it is important to investigate the temperature dependence of the oxidation properties of aluminized coatings on steel with high concentrations of Cr. The formation of protective Al_2O_3 is expected to protect the steel substrate during high temperature service. The phase composition and performance of the Fe-Al alloy layer are strongly affected by both the make up of the raw material and temperature treatment. Few studies have reported the combined effect of Cr concentrations on the oxidation resistance of Fe-Al based alloys at high temperatures based on long term cyclic oxidation, which relates to the resistance of the coating at high temperatures.

In this study, ferritic SS430 was coated by hot-dipping to deposit aluminum on the bare steel. The degradation of aluminide layer on the surface of steel substrate was investigated by cyclic oxidization test under a static atmosphere at 900 °C and 1000 °C. The oxidation kinetics behavior was also studied by the weight change of specimens every cycle.

RESEARCH METHOD

A commercial ferritic 430 SS sheet is used as the bare substrate. A rectangular specimen was fabricated with the dimensions of 20×10×1.5 mm^3 using a water-cooled cutting machine. Before aluminium deposition, all specimens were ultrasonically cleaned in a solution of 5% NaOH, 10% H_3PO_4, and

then coated using a uniform welding flux. The commercial pure Al was melted in an alumina crucible and maintained at a temperature of 700 °C. The specimens were dipped for 3 minutes into the molten Al bath. The oxide flux deposited on the surface of the aluminized specimens was then cleaned using a nitric acid, phosphoric acid, and water solution (1:1:1 v/v) at room temperature.

Cyclic oxidation tests were conducted at 900 °C and 1000 °C in an automatic box furnace for 350 cycles and 250 cycles, respectively. Each cycle consisted of a one-hour period at 900 °C or 1000 °C, and one-hour at room temperature. Weight changes were measured every 6 cycles with an accuracy of ±0.1 mg. The mass changes excluded the amount of oxide that was released during cooling.

The structure and phases of the specimens were identified by X-ray diffraction (XRD) using monochromatic Cu-Kα radiation at 40 kV and 100 mA. The surface morphology and cross-sections of the specimens were examined using scanning electron microscopy (SEM) with energy dispersive spectroscopy (EDS). The thickness of the aluminide layer and composition of the elements were obtained by analyzing the EDS data; the distance from the surface was then plotted as a function of the atomic compositions (at.%).

RESULT AND DISCUSSION

Microstructure and Phases as Coated Specimen

The SEM cross sectional image of the as-coated specimen is shown in Figure 1.

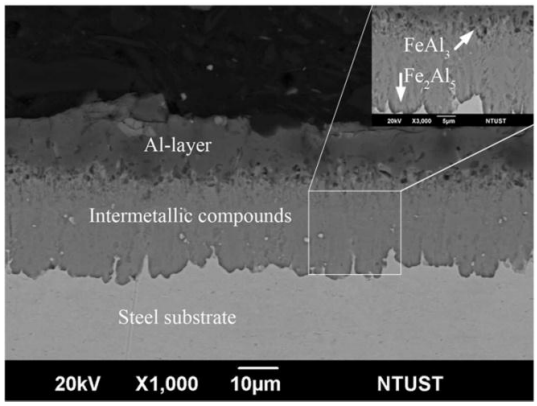

Figure 1. SEM of Cross-Sectional Micrograph of as Coated Specimen

Typically, the coating consists of two distinct layers with a total thickness of about 39.7 μm. The outer layer contains mostly aluminum and the inner layer consists of Fe-Al intermetallic compounds which form due to Fe/Al inter-diffusion during hot dipping, where the diffusivity of Al into the steel substrate is faster than the diffusivity of Fe into Al. XRD analyses identify that the aluminide layer consists of two phases, namely $FeAl_3$ and Fe_2Al_5. Based on the EDS analysis, $FeAl_3$ and Fe_2Al_5 have an elemental composition around 21.17Fe -78.03Al and 25.87Fe -74.13Al (at. %), respectively.

The columnar grain of $FeAl_3$ grew between the Fe_2Al_5 domain and the aluminum layer in which a concentration gradient of iron existed in the molten aluminum. High Cr concentration in the steel substrate results in the rough features of both phases. Furthermore, the finger-like morphology of the Fe_2Al_5 layer is irregular.

Degradation of the Aluminide Layer

In order to understand the degradation of the aluminide layer and growth of oxide during cyclic oxidation, the cross-sectional micrographs were examined using SEM and EDS for different oxidetion temperatures. Transformation of Fe_2Al_5 and $FeAl_2$ phases increased the aluminide layer thickness as temperature and time exposure was increased and formed either FeAl or Fe_3Al depending on temperature exposure. The different SEM of cross-sectional micrographs for the specimens oxidized at 900 °C and 1000 °C for 5 cycles are depicted in Figure 2.

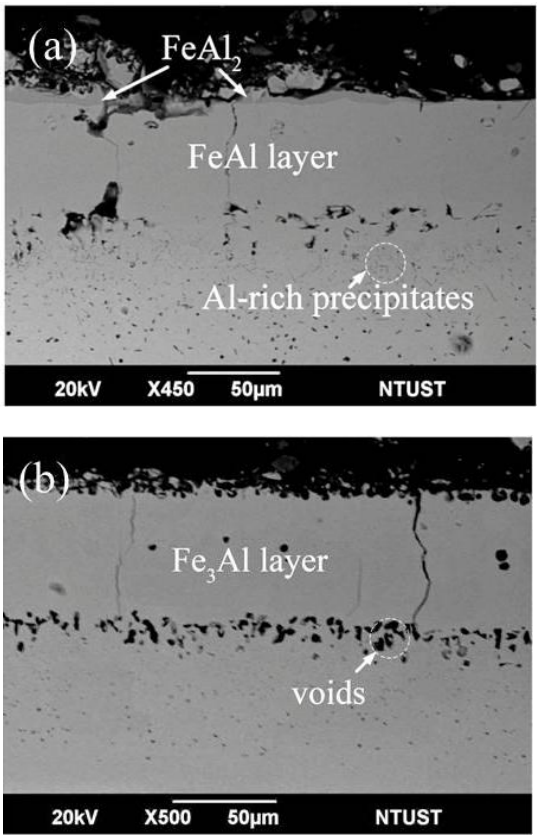

Figure 2. SEM Morphology of a Cross-Section of a Specimen Which had been Oxidized for 5 Cycles at (a) 900 °C and (b) 1000 °C

The phase formation of Fe_3Al was easily produced by controlling the phase transformation of FeAl at temperatures of greater than 900 °C [7]. In the aluminide layer containing either FeAl or Fe_3Al and some dissolved Cr, the decrease of Cr concentration in areas had given contribution to formation of micro-cracks in which Al had diffused. Jung reported a similar finding in the aluminide layer formed on TiAl alloys the number of cracks decreased with increasing the Cr content [12]. Cracks perpendicular to the surface were generated by thermal anisotropy due to changes of phase transformation in the aluminide layer. Any thermal expansion mismatch problem was attributed by the higher Al content, a thicker coating and high cycle temperature exposure. Thus, the thermal expansion coefficient of FeAl and Fe_3Al are 21.5×10^{-6}/°C and 19×10^{-6}/°C, respectively, which is much higher than that of steel substrate (11.4×10^{-6}/°C) [13].

EDS and XRD analyses show that the major phase is Fe_3Al with Cr-contents of around 10.21 (at.%) for the specimen oxidized at 1000 °C after 250 cycles, see Figure 3b and 4b.

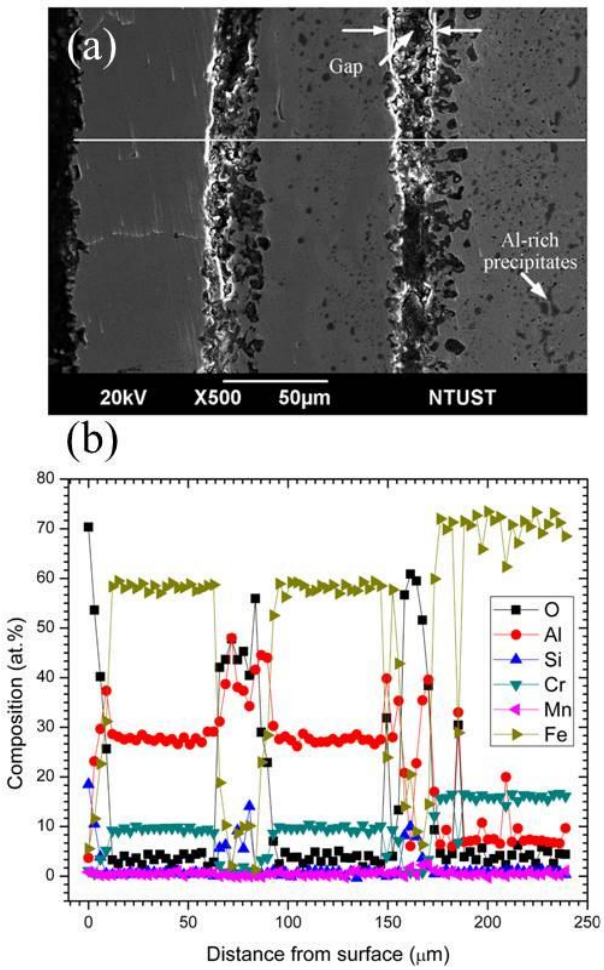

Figure 3. (a) Morphology of a Cross-Ssection and (b) EDS Line Profile of an Aluminized Specimen After 250 Oxidation Cycles at 1000 °C

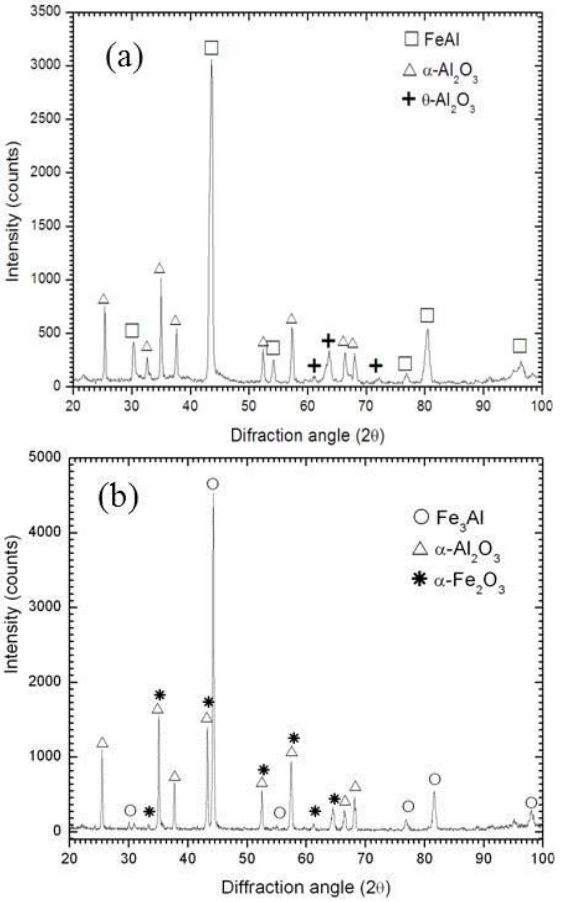

Figure 4. X-RD Diffraction Patterns of Aluminized 430 Stainless Steel After Cyclic Oxidation at (a) 900 °C and (b) 1000 °C for 350 and 250 Cycles, Respectively

Whereas, significantly different result is obtained at 900 °C; the aluminide layer mainly consists of FeAl with a Cr concentration of about 8.36 (at. %) as shown in Figure 5.

As mentioned above, the crack perpendicular to the surface of the specimen in the aluminide layer growing through surface allows oxygen to reach the inner interface of the scale via crack network [14,15]. Figure 3 and 5 show cross-sectional micrographs and the corresponding EDS line profiles of elements of oxide and aluminide layer formed after oxidation at 1000 °C and 900 °C. Both cross-sectional micrographs reveal the nonadherent, fragile oxide scales. In the present study, the spallation of oxide scale occurred not only during oxidation but also during sample handling at room temperature. Formation of voids and cavities due to the coalescence of vacancies induced by the uneven flux of anions and cations leads to the Al_2O_3 layer and aluminide layer detachment.

The inward transport of oxygen from the outer edge through cracks could repair gaps and consequently increase the partial pressure of oxygen within the gap zone. A gap formed through vacancy condensation due to the rapid growth rate of the

aluminum oxide formed at the interface. As shown in figure 3a, it was found that two aluminide layers on the specimen oxidized at 1000 °C after 250 cycles oxidation. The first aluminide layer is possibly a remnant from a partially peeled off aluminide layer, which then attached on the surface of other aluminide layers.

XRD analysis confirms that Fe_2O_3 is only found at 1000 °C, whereas Cr_2O_3 is not found. This result is evident with SEM observation of surface morphology of the aluminized specimens after 30 cycles, as shown in figure 6. The EDS analysis clearly reveals in figure 3b that the α-Al_2O_3 scale contains a small amount of dissolved Fe-atoms because the solubility of Fe-atoms in the Al_2O_3 is about 5% at 1000 °C [10]. Perez et al. reported that at the oxidation temperature of approximately 950 °C the formation of Cr_2O_3 was restricted by the formation of volatile CrO_3 [16]. However, the EDS analysis only detects a little chromium; this means that the presence of Cr may promote aluminum diffusion, which then forms aluminum oxide in the gap. Whereas, Fe_2O_3 and Cr_2O_3 are not found in the specimens oxidized at 900 °C, see Figure 7.

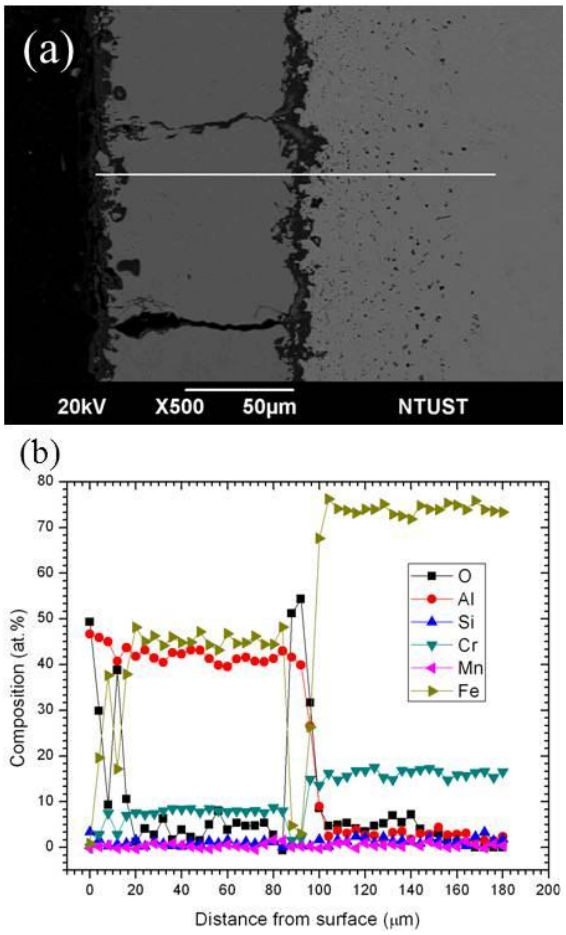

Figure 5. (a) SEM of Cross-Section Micrograph and (b) EDS Line Profile of The Aluminized Specimen after 350 Oxidation Cycles at 900 °C

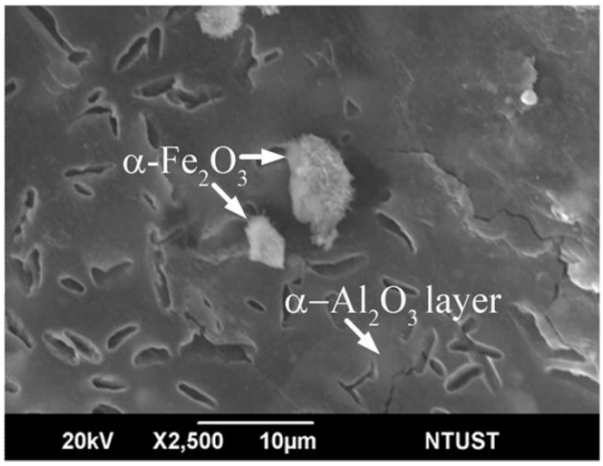

Figure 6. SEM of Surface Morphology of Aluminized 430 SS After 30 Cycles at 1000 °C

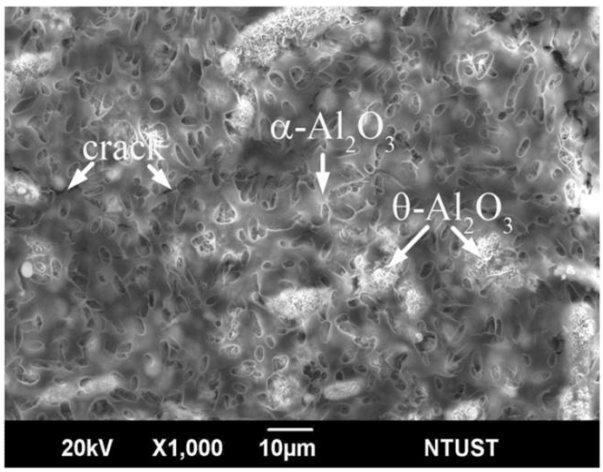

Figure 7. SEM of Surface Morphology of Aluminized 430 SS After 350 Cycles at 900 °C

Meta-stable transient θ-Al_2O_3 was found growing underneath α-Al_2O_3 in figure 7 and EDS detects both Fe and Cr atoms, as shown in figure 5b. These results are consistent to be reported by Lee et al. that Fe and Cr atoms from the aluminide layer could give a contribution to support a formation of the α-Al_2O_3 layer [10]. Both Fe and Cr are well known to accelerate the transformation of θ-Al_2O_3 to α-Al_2O_3 [17-19]. The meta-stable transient of θ-Al_2O_3 has a whisker-like morphology, whereas α-Al_2O_3 is observed as a dense layer. In addition, θ-Al_2O_3 has a lower density than α-Al_2O_3 and the transformation is accompanied by a 13% volume reduction [20] which is a cause of cracks in the outer region. The higher growth rates of meta-stable oxides are related to their crystal structures and looser packing arrangements than α-Al_2O_3 (which has a hexagonal close-packed oxygen structure with aluminum occupying octahedral interstitial sites). The different morphologies developed by the alumina phases also contribute to their differing growth rates.

Effect of Temperature with Respect to Cyclic Oxidation Kinetics

A cyclic oxidation test was carried out to evaluate the resistance of the aluminide coating under cyclic thermal stress. The weight change versus cycles curve at 900 °C and 1000 °C is shown in figure 7. Similar trends are observed over 30 cycles: 1.9 mg/cm^2 and 2.4 mg/cm^2 for the specimens oxidized at 900 °C and 1000 °C, respectively. The weight change of a specimen oxidized at 1000 °C shows an abnormal increase that is followed by a rapid decrease during 50–160 cycles because some parts of the aluminide layers and alumina oxide break and peel off the steel substrate. However, after reaching 160 cycles, weight change undergoes a constant rate. Montealegre et al. suggested that the magnitude of the area the peeled off aluminide layer depends on the magnitude of thermal stress resulted from interaction between aluminum oxide and aluminide layer [21]. In addition, the existence of thermal stress in the aluminum oxide at high temperatures can cause creep of the scale in the underlying aluminide layer, depending on the relative thickness of the aluminide layer and oxide layer [22].

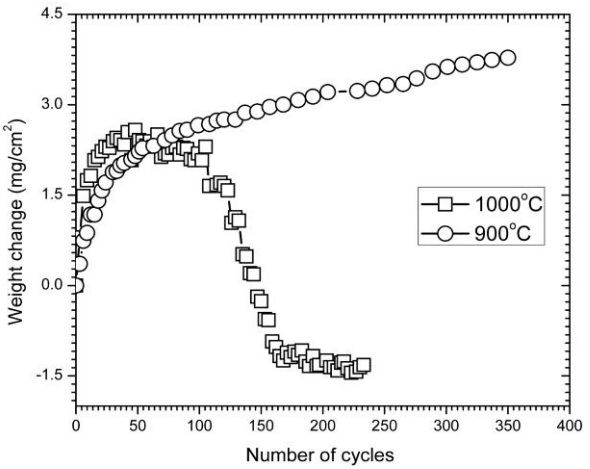

Figure 8. The Kinetics Curve of Aluminized SS430 Under Cyclic Thermal Oxidation

As time exposure is increased, some cracking and spallation of the alumina layer occurs due to the rapid growth of α-Al_2O_3 in the outer scale region at 1000 °C. The specimen oxidized at 900 °C still exhibits a sequence of weight changes over 350 cycles.

CONCLUSSION

The cyclic oxidation in static air of hot-dipped aluminized ferritic 430 SS was performed at 900 °C and 1000 °C. Aluminum in the topcoat completely diffused into the steel substrate to form intermetallic compounds which varied based on the treatment temperature. The Fe_2Al_5 and $FeAl_2$ rapidly transformed into the FeAl and Fe_3Al owing to aluminum diffusion for short time oxidation at the different temperature service. The crack perpendicular to the surface of specimens was incorporated by a thermal expansion mismatch, generating a tensile stress and then induced rapidly into micro-crack in the aluminide layer during cooling. The accumulation of voids generates a crack at the interface; consequently new alumina oxide formed within the crack, allowing some level of self repair. In the present study, it shows that the high solubility of chromium (up to 10.21%) is detrimental to the oxidation resistance of aluminized 430 stainless steel at 1000 °C, leading to an overall higher parabolic rate constant under cyclic oxidation thermal.

REFERENCES

1. Saeki, I., Konno, H., Furuichi, R., Nakamura, T., Mabuchi, K. and Itoh**,** M., *Initial Oxidation of Type 430 Stainless Steel in O_2-H_2O-N_2 Atmospheres at 1273 K*, Corr. Sci. 38(1), pp. 19–31, 1996.
2. Galerie, A., Wouters, Y.S., Pijolat, M.L., Valdivieso, F., Soustelle, M., Magnin, T., David, D., Bosch, C. and Bayle, B., *Mechanisms of Corrosion and Oxidation of Metals and Alloys*, Edv. Eng. Mater, 3(8), pp. 555–561, 2001.
3. Dah, E.N., Tsipas, S., Hiero, M.P. and Perez, F. J., *Study of The Cyclic Oxidation Resistance of Al Coated Ferritic Steels with 9 and 12% Cr*, Corr. Sci, 49, pp. 3850–3865, 2007.
4. Chang, Y.Y., Tsaur, C.C. and Rock, J.C., *Microstructure Studies of an Aluminide Coating on 9Cr–1Mo Steel During High-Temperature Oxidation,* Surf. Coat. Technol, 200(65), pp. 88–93, 2006.
5. Wang, C.J., Lee, J.W. and Twu, T.H., *Corrosion Behaviors of Low Carbon Steel, SUS310 and Fe–Mn–Al Alloy with Hot-Dipped Aluminum Coatings in NaCl–Induced Hot Corrosion*, Surf. Coat. Technol., 163–164, pp. 37–43, 2003.
6. Wang, C.J. and Chen. S.M., *The High-Temperature Oxidation Behavior of Hot-Dipping Al-Si Coating on Low Carbon Steel*, Surf. Coat. Technol., 200, pp. 3862–3866. 2006.
7. Kobayashi, S. and Yakou, T., *Control of Intermetallic Compound Layers at Interface Between Steel and Aluminum by Diffusion-Treatment*, Mater. Sci. Eng. A., 338, pp. 44–53, 2002.
8. Yu, X. and Sun, Y., *The Oxidation Improvement of Fe_3Al Based Alloy with Cerium Addition at Temperature Above 1000°C,* Mater. Sci. Eng. A, 363(1–2), pp. 30–39, 2003.

9. Lee, K.S., Oh, K.H., Park, W.W. and Ra, H.Y., *Growth of Alumina Oxide Film in High Temperature Oxidation of Fe–20Cr–5Al Alloy Thin Strip,* Scripta Materialia, 39(8), pp. 1151–1155, 1998.

10. Lee, D.B., Kim, G. Y. and Kim, J.G., *The Oxidation of Fe_3Al–(0, 2, 4, 6%)Cr Alloys at 1000°C*, Mater. Sci. Eng. A, 339(1–2), pp. 109–114, 2003.

11. Velon, A. and Yi, D.Q., *Influence of Cr on The Oxidation of Fe_3Al and Ni_3Al at 500°C, Oxid.* Met. 57(1–2), pp. 13–31, 2002.

12. Jung, H.G., Jung, D.J. and Kim, K.Y., *Effect of Cr on The Properties of Aluminide Coating Layers Formed on TiAl Alloys*, Surf. Coat. Technol., 154, pp. 75–81, 2002.

13. Meyers, M. and Chawla, K., *Mechanical Behavior of Materials*, second ed., Cambridge University Press, New York, 2009.

14. Cheng, W.J. and Wang, C.J., *Growth of Intermetallic Layer in The Aluminide Mild Steel During Hot-Dipping*, Surf. Coat. Technol., 204, pp. 824–828, 2009.

15. Wang, C.J., and Badaruddin, M., *The Dependence of High Temperature Resistance of Aluminized Steel Exposed to Water-Vapour Oxidation*, Surf. Coat. Technol., 205, pp. 1200–1205, 2010.

16. Perez, F.J., Hierro, M.P., Pedraza, F., Carpintero, M.C., Gomez, C. and Tarin, R., *Effect of Fluidized Bed CVD Aluminide Coatings on The Cyclic Oxidation of Austenitic AISI 304 Stainless Steel*, Surf. Coat. Technol., 145(1–3), pp. 1–7. 2001.

17. Bye, G.C. and Simpkin, G.T., *Influence of Cr and Fe on Formation of α-Al_2O_3 from γ-Al_2O_3,* J. Am. Ceram. Soc., 57, pp. 367–371, 1974.

18. Choi, S.C., Cho, H.J. and Lee, D.B., *Effect of Cr, Co, and Ti Additions on The High-Temperature Oxidation Behavior of Ni_3Al*, Oxid. Met., 46, pp. 109–127, 1996.

19. Pint, B.A., Martin, J.R. and Hobbs, L.W., *The Oxidation Mechanism of θ-Al_2O_3 Scales*, Solid State Ionics, 78, pp. 99–107, 1995.

20. Young, D.J., *High Temperature Oxidation and Corrosion Metals*, first ed., Elsevier, Amsterdam. 2008.

21. Montealegre, M.A., Gonzales, C.J.L., Morris, M. M.A., Chao, J. and Morris, D.G., *High Temperature Oxidation Behaviour of an ODS FeAl Alloy*, Intermetallics, 8(4), pp. 439–446, 2000.

22. Tolpygo, V. K. and Clarke, D. R., *Alumina Scale Failure Resulting from Stress Relaxation*, Surf. Coat. Technol., 120, pp. 1–7, 1999.